

Effective stress and water pressure in saturated clays during heating-cooling cycles¹

T. HUECKEL

School of Engineering, Duke University, Durham, NC 27706, U.S.A.

AND

R. PELLEGRINI

ISMES, 24100 Bergamo, Italy

Received June 15, 1992

Accepted June 22, 1992

Experiments with heating and cooling cycles in undrained constant total stress conditions in triaxial apparatus are presented. Heating induces a large pore-water pressure increase, which eventually leads to a large irreversible strain and possible mechanical failure. Subsequent cooling produces a drop in water pressure. In one test the drop during cooling was more than two times higher than the previous increase during heating, reaching values of up to 2.30 MPa. An analysis of these findings in terms of a thermoplastic model is presented. The interpretation of these tests relies heavily on the kind of stress-partitioning hypothesis that is used. It was found that the described phenomena can be quantitatively dealt with using the classical effective stress principle, if the shear strength and consolidation are described in terms of temperature-dependent plastic yield limit.

Key words: temperature, plastic strains, effective stress, pore pressure.

Des expériences avec des cycles de chauffage et de refroidissement produits dans l'appareil triaxial dans des conditions non drainées en contrainte totale constante sont présentées. Le chauffage induit une augmentation importante de la pression interstitielle qui conduit éventuellement à une grande déformation irréversible et possiblement à une rupture mécanique. Le refroidissement subséquent produit une chute dans la pression interstitielle. Dans un essai, la chute durant le refroidissement était plus de deux fois plus importante que l'accroissement antérieur durant le chauffage, atteignant des valeurs jusqu'à 2,30 MPa. L'on présente une analyse de ces résultats en fonction d'un modèle thermo-plastique. L'interprétation de ces essais dépend fortement de l'hypothèse de partition de contrainte utilisée. L'on a trouvé que, si la résistance au cisaillement et la consolidation sont décrites en fonction de la limite de déformation plastique dépendante de la température, les phénomènes décrits peuvent être traités quantitativement en utilisant le principe des contraintes effectives classique.

Mots clés : température, déformations plastiques, contrainte effective, pression interstitielle.

[Traduit par la rédaction]

Can. Geotech. J. 29, 1095-1102 (1992)

Introduction

This paper deals with cycles of heating and cooling of clay in undrained conditions. It is a continuation of previous work which focused on the response of clay mass to monotonic heating. Constant total stress undrained heating-cooling tests on saturated clays published previously are analysed. This sort of cyclic testing simulates thermomechanical behavior of clay around a heat source like a nuclear-waste repository. Nuclear waste has a decaying heat output. This leads to an initial increase of temperature in the soil mass after installation, followed by its gradual decrease (see, for example, Pellegrini *et al.* 1989). The former experiments (Hueckel and Pellegrini 1989, 1991) indicated failure of specimens at 70–92°C, under total stress conditions considered as absolutely stable mechanically. The new results concerning monotonic heating in this paper are compared with the previous findings to seek a confirmation of the suggested interpretation. Numerical simulations using thermoplasticity theory are then compared with the test results. Finally, a theoretical interpretation is given to the results of the cyclic

thermal testing published previously by Hueckel and Pellegrini (1989).

The interpretation of the discussed tests depends on the hypothesis adopted on stress partitioning. It was found that the described phenomena can be quantitatively dealt with using the classical effective stress principle, if the shear strength and consolidation are described in terms of a temperature-dependent plastic yield limit.

Thermal failure in sands was observed by Agar *et al.* (1986) and suggested as a possible failure mechanism in ocean-floor sediments by Davis and Banerjee (1980).

Experimental

Two clays were subjected to cyclic heating tests: Boom clay from 240 m depth at Mol, Belgium; and Pasquasia clay from 160 m depth in Sicily, Italy. Boom clay is relatively soft and highly plastic (22% smectite, 19% illite, 29% kaolinite), with a low water content. Pasquasia clay is a medium-plasticity cemented clay, sometimes fissured, with 10–15% kaolinite, <5% smectite, 20–25% calcite, 15–20% quartz, and with a very low (13%) water content and low permeability. The tests were performed at ISMES with the high-pressure, high-temperature triaxial apparatus shown in Fig 1.

¹Paper presented at the workshop on "Stress Partitioning in Engineered Clay Barriers," May 29–31, 1991. Duke University, Durham, N.C.

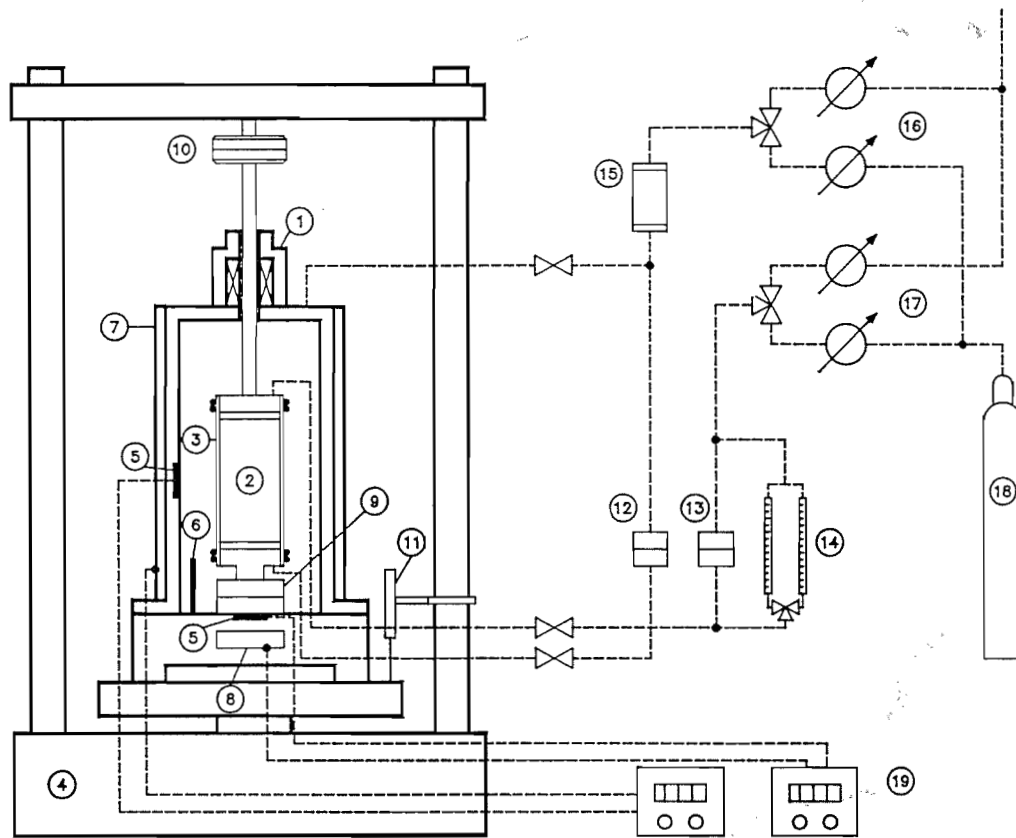


FIG. 1. Schematic of ISMES experimental setup. 1, triaxial cell; 2, specimen; 3, membrane; 4, press (load and speed controlled); 5, heater thermocouples; 6, main thermocouple; 7, lateral heater; 8, bottom heater; 9, internal load cell; 10, external load cell; 11, LVDT (axial deformation measurements); 12, differential pressure transducer (effective stress); 13, differential pressure transducer (volume change); 14, burette (volume-change measurements); 15, air-water interface; 16, cell pressure regulator; 17, back-pressure regulator; 18, nitrogen bottle, 19, data acquisition set.

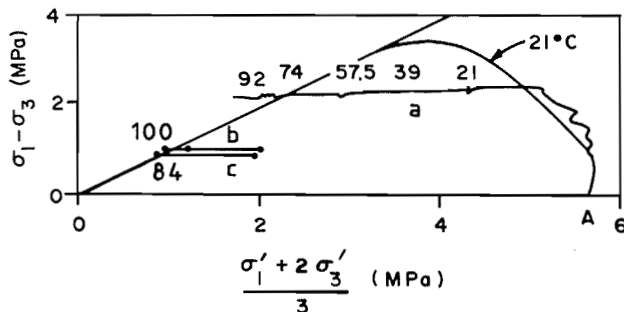


FIG. 2. Effective stress paths for Boom clay. *a*, test TBoom 2; *b*, test TBoom 12; *c*, test TBoom 14.

The experiment consisted in heating of clay specimens under undrained conditions at a constant total nonisotropic stress state. In the case of Boom clay, three total stress states were examined: an anisotropically normally consolidated state and two overconsolidated states. Pasquasia clay was investigated in an overconsolidated state.

After the desired total stress level was attained, the material was allowed to develop undrained creep up to a stabilization of pore pressure at room temperature. Heating was then performed at closed drainage in small temperature steps. Because the testing system, including the cell, water tubings, and porous stones, was subjected to thermal expansion, corrections were applied by a release of calibrated quantities of water. This has been adopted to simulate actual undrained

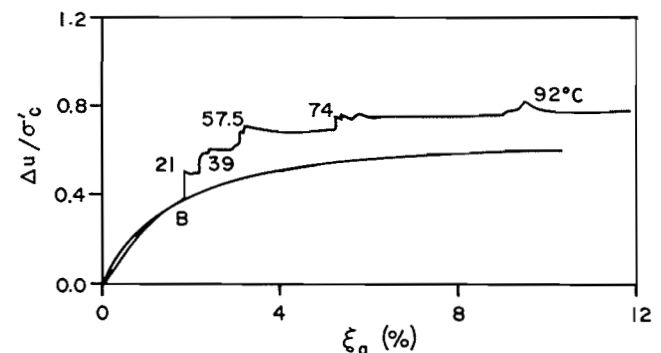
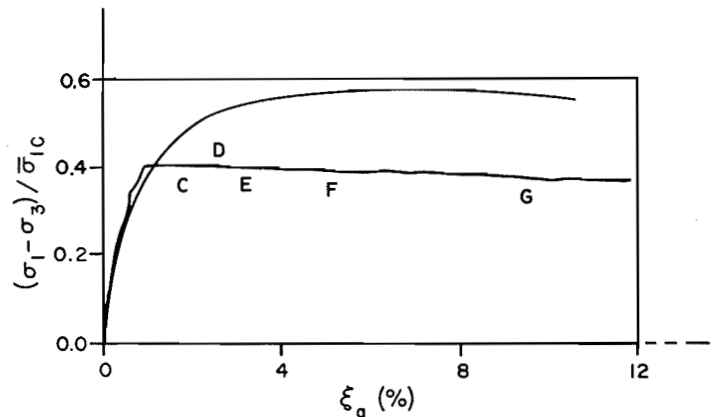


FIG. 3. Normalized water pressure vs. axial strain for applied temperature steps B-G in test TBoom 2.

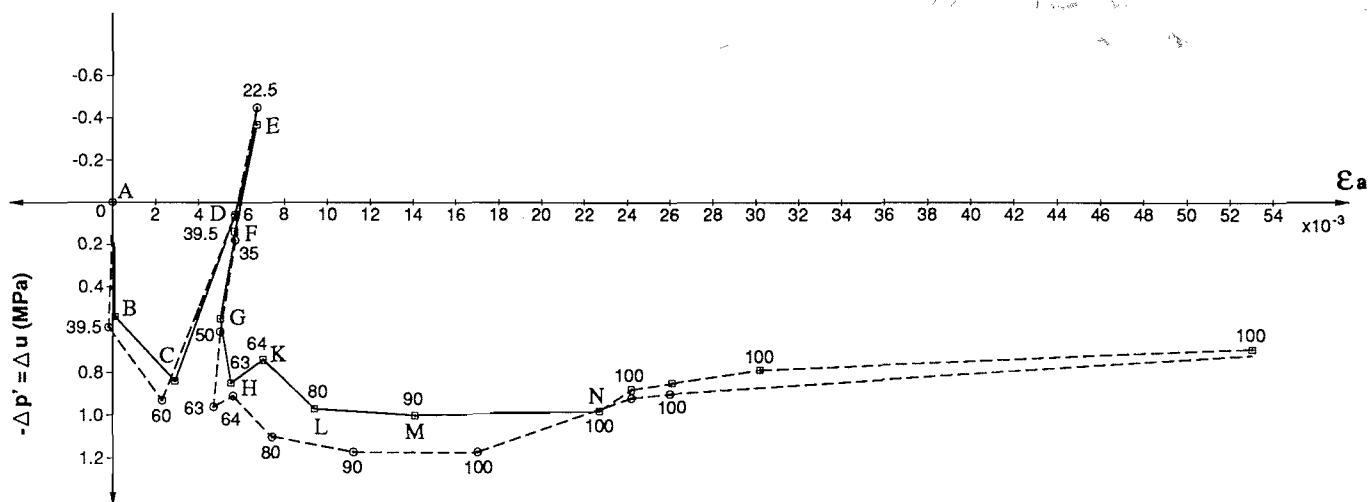


FIG. 4. Pore-water pressure vs. axial deformation in undrained test TBoom 12 for applied temperature steps (A-H, K-N; temperatures in °C) at constant total stress ($q = 0.94$; $p = 2.00$ MPa). \odot , immediate; \square , long term.

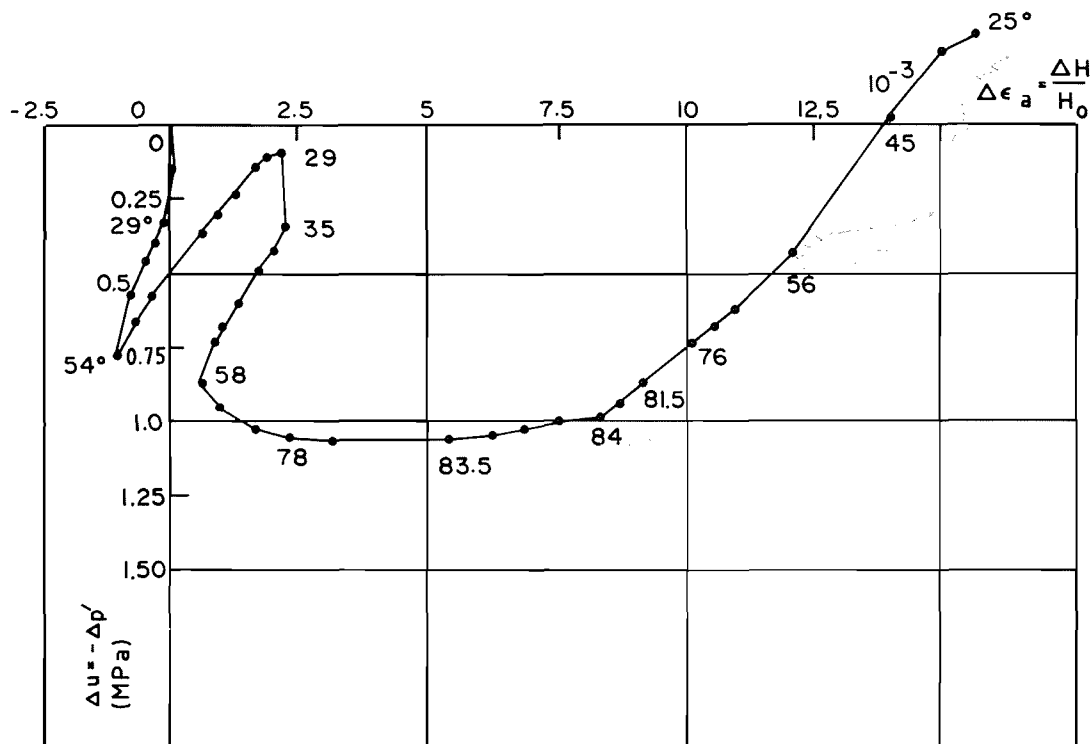


FIG. 5. Pore-water pressure vs. axial deformation in undrained test TBoom 14 for applied temperature steps (°C) at constant total stress ($q = 1.0$; $p = 1.98$ MPa).

conditions in the sample, as an extreme case of *in situ* conditions. The corrections were not applied in the first test on Boom clay. Thermal strain, which is usually much smaller than mechanically induced strain, was measured using an alternative (thinner) burette system.

Results

Some results of monotonic heating of an anisotropically, normally consolidated Boom clay specimen (test TBoom 2) were presented previously (Baldi *et al.* 1988; Hueckel and Pellegrini 1989, 1991). The new results presented here allow us to derive some basic conclusions on thermomechanical failure of clays. In the first test (Hueckel and Pellegrini 1989) a specimen at 21°C was isotropically consolidated at

5.75 MPa, then subjected in undrained conditions to the stress difference of 2.0 MPa and allowed to creep until stabilization of water pressure. Subsequently, the specimen was heated in undrained conditions at constant total stress. The effective stress path, calculated according to Terzaghi's effective stress principle from the pore-water pressure readings, is shown in Fig. 2 (path *a*). Ambient temperature undrained triaxial compression stress path for the same clay is included for comparison. In Fig. 3 the development of pore-water pressure, normalized with respect to the confinement stress, $\sigma'_c = 5.75$ MPa, is presented versus axial strain. It is seen that the water-pressure growth during heating is substantial. At 74°C the rate of axial strain per grade is already high. Failure occurred at 92°C ($\Delta T =$

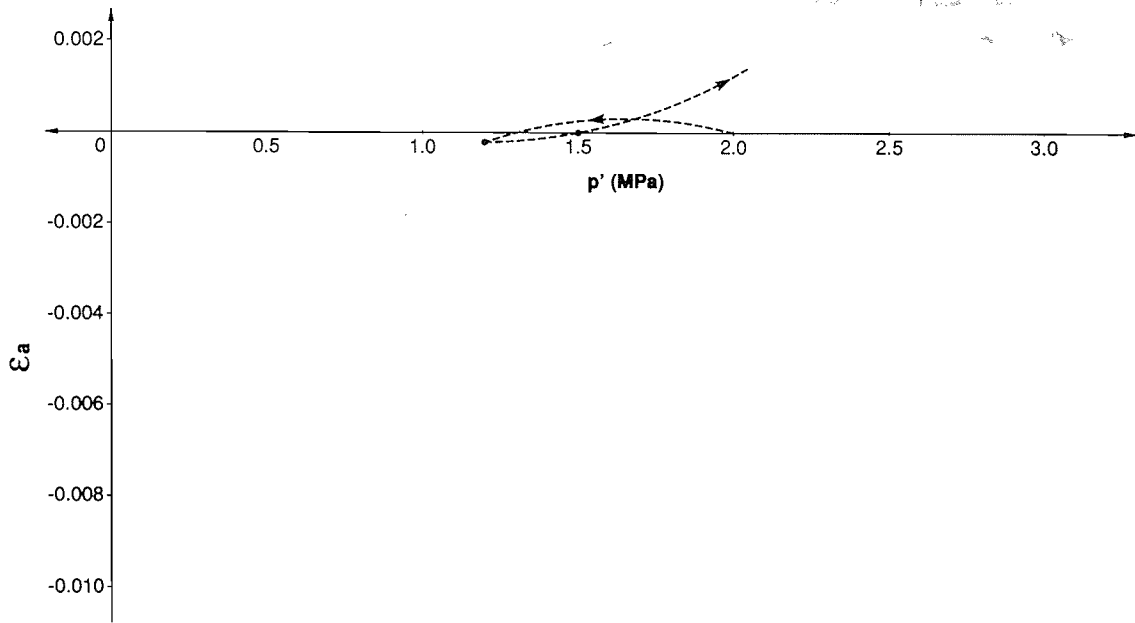


FIG. 6. Axial strain versus isotropic effective stress during purely mechanical test of isotropic unloading/reloading, at constant deviator stress $q = 1.0$ MPa, to simulate mechanical strain in test TBoom 14.

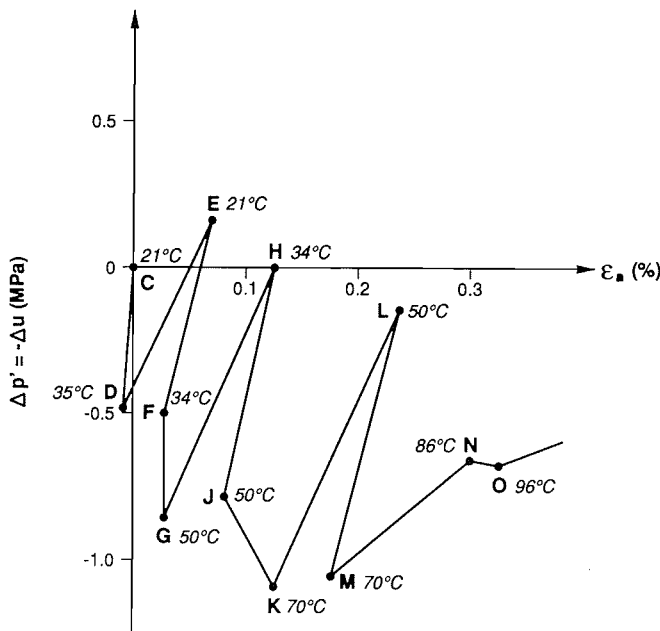


FIG. 7. Pore-water pressure vs. axial deformation in undrained test TPas 9 for applied temperature steps at constant total stress ($q = 2.00$; $p = 3.00$ MPa).

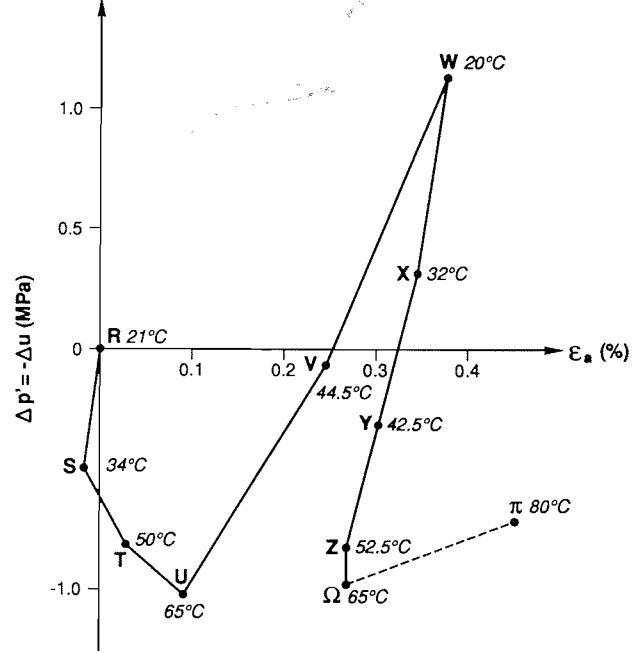


FIG. 8. Pore-water pressure vs. axial deformation in undrained test TPas 10 for applied temperature steps at constant total stress ($q = 2.00$; $p = 3.00$ MPa).

71°C), with $\Delta u = 4.01$ MPa at 1.61 MPa of effective mean stress. A shear band was detected in the specimen after the test completion.

New experiments were performed on overconsolidated specimens of Boom clay (tests TBoom 12 and 14) at different constant total stress. The stress paths are marked in Fig. 2 as *b* and *c*. During test TBoom 12, at the stress difference of 0.9 MPa and total isotropic stress of 2.0 MPa, a heating-cooling-reheating cycle, 22.5–60–22.5–100°C, was performed. Axial deformation versus change in effective mean stress is shown in Fig. 4. While an increase of water pressure of 0.86 MPa was reached during heating from 22.5 to 60°C, the drop during cooling was much higher (1.25 MPa), and

almost identical to it was the increase in Δu during the second heating from 22.5 to 60°C. A dramatic increase in axial strain up to 5.4% was observed starting from 64°C, followed by stabilization and then by a slight drop in the pore-water pressure (over 0.45 MPa).

Test TBoom 14 was essentially following the program of test TBoom 12 (see Fig. 2, path *c*), with the important difference that cooling was initiated at a lower temperature, viz. 54°C. During cooling to 29°C, a much smaller drop in water pressure occurred (Fig. 5) compared with TBoom 12.

In addition, a mechanical test at the same constant total stress was conducted for comparison. The purpose of the

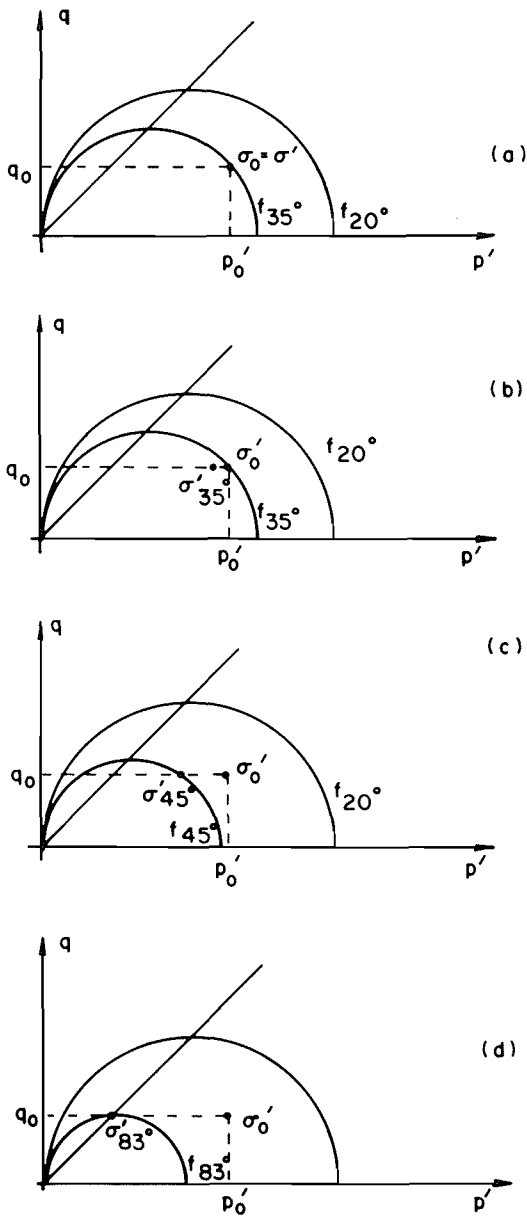


FIG. 9. Schematic of the thermal dependence of the yield locus f , in (a) drained and (b-d) undrained TBoom 14 heating tests.

test was to evaluate the strain produced during isotropic unloading and reloading along the same stress path as in the thermal part of the experiment. In this test, pore-water pressure was forced mechanically through variations of the back pressure. The total stress was equal to that in tests TBoom 12 and TBoom 14. The results are presented in Fig. 6 in terms of axial strain versus isotropic effective stress p' . When the effective stress of 1.2 MPa is reached, a much smaller tensile axial strain is observed, compared with that produced by the same effective stress change induced by heating. Finally, upon reloading to 2 MPa, the permanent compressive axial strain is smaller again (1.76‰) than the thermal strain obtained in TBoom 12.

In the tests on Pasquasia clay the initial stress state of deviatoric stress $q = 2.0$ MPa and of isotropic stress $p' = 3.0$ MPa was reached in drained loading. The vertical *in situ* precompression stress was estimated as equal to 17.0 MPa, thus the overconsolidation ratio (OCR) was about 7.22. The

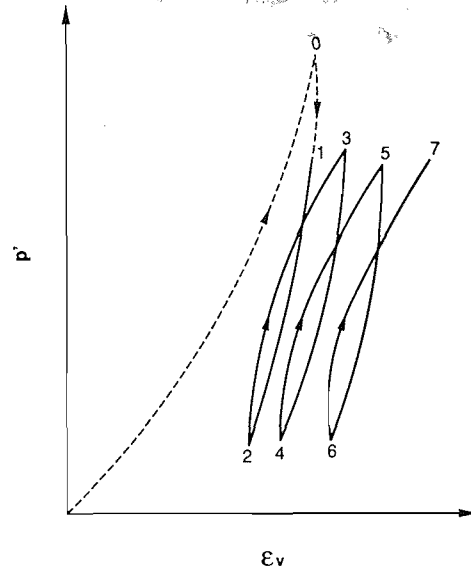


FIG. 10. Schematic of isotropic stress-strain loading-unloading-reloading response.

two tests were similar. Where the conditions in the two tests overlapped, the results were very similar. The undrained response to thermal loading of test TPas 9 is presented in Fig. 7, which gives pore-pressure change versus vertical strain for the applied temperature steps. An analogous plot for test TPas 10 is shown in Fig. 8.

In test TPas 9, the axial strain during the first heating step was expansive, whereas cooling led to a substantially larger compaction, producing 0.8 ‰ of irreversible axial strain. Reheating up to 34°C produced a larger expansion than the first heating; however, a net accumulation of the compressive axial strain of 0.125‰ was generated during the cycle 21–35–21–34°C. Further heating up to 50°C produced no axial strain, whereas the water pressure increased to 0.8 MPa. Subsequent cooling back to 34°C shows a significant axial compaction on that cycle and pore-pressure reduction to zero at 34°C. In the cycles up to 70°C a regularity of strain development may be seen in that all the cooling portions of $\Delta p'$ versus $\Delta \epsilon_a$ are parallel. The same refers to the reheating portions. Virgin heating portions, e.g., J–K, M–N, produced more and more compressive axial strain.

Comparing tests TPas 10 and TPas 9 it may be concluded that the progressive compression by heating observed in TPas 10 is not affected by the cooling–reheating cycles performed in test TPas 9. A high 1.18 MPa negative residual pore-pressure difference remaining after cooling is the most important observation from test TPas 10. Heating above 70°C produced a decrease in water pressure of about 0.25 MPa. Water pressure stabilized at about 0.75 MPa in both tests, at 80–90°C.

It must be emphasized that all elements of the apparatus were very carefully checked to be sure that any water-pressure drop was due to the behavior of the specimen and not due to the equipment itself. Major membrane leaks can be excluded. The least sensitive membrane (bromide butyl) was selected for the above study (Baldi *et al.* 1991). A leak would lead to an inverse liquid flow, i.e., toward the specimen, and thus would increase the pore pressure. The cell liquid was silicon oil, and no trace of this liquid was found in the specimen after completion of the test. Finally, in

tively, from Fig. 7, whereas reloadings 2-3, 4-5, and 6-7 correspond to those in D-E, H-G, and K-L. All but the first unloading portions of the plot in Fig. 7 are parallel to each other. The same refers to the reloading portions. This confirms a one-to-one stress-strain dependence in this range. Besides the effects of the cyclic strain accumulation D-F, or G-J in the thermal cycling test (corresponding to 2-4 and 4-6 in Fig. 10), there are plastic yielding portions F-G, J-K, and M-N, where the effective stress point reenters in contact with the thermally shrinking yield surface. Each plastic portion is characterized by an enhanced vertical compression, when compared to analogous elastic portions, as visualized in the yield surface history diagram (Fig. 11). Finally, at $\Delta p' = 1.2$ MPa the growth of water pressure ceases, despite the temperature growth. This occurs where the effective stress path reaches the critical state.

The following observations may be made at this point. First, the thermal dependence of the yield surface is symmetric with respect to heating and cooling. This may be inferred from the fact that yielding points J and M at 50 and 70°C are at about the same effective stress as points G and K, respectively, at yielding prior to the cooling-heating cycle. The same refers to points Ω and U for test TPas 10 (Fig. 8). Second, the effective stress decrease in the plastic process, like F-G from 34 to 50°C (Fig. 7) is much smaller than that in an analogous elastic one like H-J. The same occurs for J-K from 50 to 70°C in comparison with L-M and in TPas 10 (Fig. 8) for S-T (34-50°C) versus X-Z (32-52.5°C). This corroborates the hypothesis that in the plastic process the shrinking of the yield surface due to temperature is slowed down by a strain hardening, which does not occur during the elastic portions.

Moreover, it is realized that a smaller decrease of the effective stress at F-G implies also a smaller elastic volumetric expansion. This means that to accommodate the thermal volumetric expansion of water, which is the same in F-G and H-J for the same temperature difference, a plastic thermal dilatancy was needed in F-G to ensure the consistency of volume. Despite this dilatancy, a strain hardening still occurs, contrasted by a thermal softening that is larger. An analogous situation takes place at J. Also, larger amounts of axial compressive strain for J-K in comparison with that in F-G indicates an increasing plastic deformation with temperature.

The actual reason for this plastic dilatancy is unknown. It may be speculated that cavitation or hydraulic fracturing occurs, noting that the water pressure is quite high (see e.g., Bjerrum *et al.* 1972). Some fracturing during heating experiments was reported by Tassoni (1980). The growing contribution of plastic dilatancy to accommodate the water expansion results in a significant residual effective stress on the closure of the cycle by cooling. Physically this means that during heating the skeleton suffers an irreversible dilatancy, which is not totally compensated for by the thermal compression occurring during elastic cooling. The remaining dilatancy induces the development of a negative pore-pressure difference. The largest (2.2 MPa) drop in water pressure giving rise to a residual negative pressure difference of 1.2 MPa, if calculated with respect to the original water pressure, is produced by heating-cooling cycle R-U-W in test TPas 10 (Fig. 8). Such a drop upon cooling may be of practical importance for the flow patterns of underground water. This means that during the cooling phase of nuclear waste, the

hydraulic gradient may be dramatically different from those during heating and should be carefully investigated.

Conclusions

From the experiments with cyclic undrained heating and cooling of saturated clays it appears that upon the completion of the thermal cycle a substantial negative pore-pressure difference may be induced in clay. The analysis based on a thermoplastic model suggests that the negative pressure is caused by a large plastic dilatancy occurring at effective stress states close to the critical state.

From the point of view of the stress-partitioning hypothesis, it should be underlined that the state of failure reached in the tests was exactly following the calculation based on the classical effective stress principle.

If any contribution from an electrochemical force change due to heating was present, it must have been of the order of the experimental accuracy.

Acknowledgements

The authors are indebted to Mr. Guiseppe Angeloni, a technician at ISMES, who performed the tests with great commitment. The work at ISMES has been carried out as part of a research program supported by the National Board of Electricity of Italy, the National Board for Alternative Energy of Italy and the Commission of European Communities.

- Agar, J.G., Morgenstern, N.R., and Scott, J.D. 1986. Thermal expansion and pore pressure generation in oil sands. *Canadian Geotechnical Journal*, **23**: 327-333.
- Baldi, G., Hueckel, T., Peano, A., and Pellegrini, R. 1991. Developments in modeling of thermo-hydro-geomechanical behaviour of Boom clay and clay based buffer materials. ISMES Commission of European Communities Report EUR 13365, vols. 1 and 2 EN, ECSC-EEC, Brussels.
- Baldi, G., Hueckel, T., and Pellegrini, R. 1988. Thermal volume changes of the mineral-water system in low-porosity clay solids. *Canadian Geotechnical Journal*, **25**: 807-825.
- Bjerrum, L., Nash, J.K.T.L., Kennard, R.M., and Gibson, R.E. 1972. Hydraulic fracturing in field permeability testing. *Géotechnique*, **22**: 319-332.
- Davies, T.G., and Banerjee, P.L. 1980. Constitutive relationships for ocean sediments subjected to stress and temperature gradients. AERE Harwell Report No. HL 80/2604 (C22).
- Hueckel, T., and Baldi, G. 1990. Thermoplasticity of saturated clays: experimental constitutive study. *ASCE Journal of Geotechnical Engineering*, **116**: 1778-1796.
- Hueckel, T., and Borsetto, M. 1990. Thermoplasticity of saturated soils and shales: constitutive equations. *ASCE Journal of Geotechnical Engineering*, **116**: 1765-1777.
- Hueckel, T., and Pellegrini, R. 1989. Modeling of thermal failure of saturated clays. *In Numerical models in geomechanics. Edited by S. Pietruszczak and G.N. Pande*, Elsevier, London, pp. 81-90.
- Hueckel, T., and Pellegrini, R. 1991. Thermoplastic modelling of undrained failure of saturated clay due to heating. *Soils and Foundations*, **31**(3): 11-16.
- Hueckel, T., Borsetto, M., and Peano, A. 1987. Thermo-elastoplastic-hydraulic response of clays subjected to nuclear waste heat. *In Numerical methods in transient and coupled problems. Edited by R.W. Lewis, E. Hinton, P. Bettess, and B.A. Schrefler*. John Wiley & Sons Ltd., Chichester, U.K., pp. 213-235.

Pellegrini, R., Borsetto, M., Peano, A., and Tassoni, E. 1989. Factors affecting the thermo-hydro-mechanical response of clay in the safety assessment of nuclear waste repositories. *In* Excavation responses in deep radioactive waste repositories—implications for engineering design and safety performance. Proceedings, OECD (Paris) Nuclear Energy Agency Workshop, Winnipeg, Man., 1988, pp. 501-514.

Tassoni, E. 1980. An experiment on the heat transmission in a clay rock. *In* The use of argillaceous materials for the isolation of radioactive waste. Proceedings, OECD (Paris) Nuclear Energy Agency Workshop, Paris, 1979, pp. 23-45.

Water uptake and swelling properties of unsaturated bentonite buffer materials¹

T. KANNO

Research Institute, Ishikawajima-Harima Heavy Industries Co., Ltd., 1, Shin-Nakahara-cho, Isogo-ku, Yokohama 235, Japan

AND

H. WAKAMATSU

Nuclear Power Division, Ishikawajima-Harima Heavy Industries Co., Ltd., 2-16, Toyosu 3-Chome, Koto-ku, Tokyo 135, Japan

Received September 3, 1991²

Accepted August 10, 1992

The water diffusivity and the development of swelling pressure are investigated in buffer materials to be used for the geologic disposal of high-level radioactive waste during the stage of unsaturated water uptake. Highly compacted blocks of Japanese Na bentonite and a bentonite-sand mixture are used as the buffer material. The water diffusivity of the blocks has turned out to be approximately equal to that of Wyoming bentonite MX-80. Assuming that the local swelling pressure in a small element of a confined bentonite mass is proportional to the degree of saturation of the local area, an elastic model with an apparent Young's modulus is developed for the first step. According to this model, the swelling pressure of the bentonite mass as a whole is proportional to the average degree of saturation of the mass. For the development of the swelling pressure in the blocks, the calculated curve by this model is in good agreement with the experimental results except during the early parts of the process.

Key words: bentonite, water uptake, water diffusivity, swelling pressure, elastic model, radioactive waste disposal.

La diffusivité et la développement de la pression de gonflement sont étudiés dans des matériaux tampons devant être utilisés pour l'entreposage géologique de résidus hautement radioactifs au cours du stade de retour d'eau non saturé. Des blocs de bentonite de sodium japonaise fortement compactée et un mélange sable-bentonite sont utilisés comme matériaux tampons. La diffusivité à l'eau des blocs s'est avérée être approximativement égale à celle de la bentonite du Wyoming MX-80. Supposant que la pression locale de gonflement dans un petit élément d'une masse de bentonite confinée est proportionnelle au degré de saturation de la zone locale, un modèle élastique a été développé pour la première étape avec un module apparent de Young. D'après ce modèle, la pression de gonflement de la masse de bentonite est globalement proportionnelle au degré moyen de saturation de la masse. Pour le développement de la pression de gonflement dans les blocs, la courbe calculée par de modèle montre une bonne concordance avec les résultats expérimentaux, sauf au cours de la période du début du processus.

Mots clés : bentonite, retour d'eau, diffusivité à l'eau, pression de gonflement, modèle élastique, entreposage de résidus radioactifs.

[Traduit par la rédaction]

Can. Geotech. J. 29, 1102-1107 (1992)

Introduction

Many countries are planning disposal of high-level radioactive wastes, including spent nuclear fuels and vitrified waste, in deep geologic formations after initial cooling. In most high-level radioactive waste repository concepts, wastes are enclosed in the waste container, and the buffer material is emplaced between the container and the surrounding host

rock. Required functions of the buffer material are as follows: (i) delay the movement of groundwater that intrudes into the repository and reaches the container, thereby delaying the time of corrosion of the waste containers; (ii) delay the migration of radionuclides from the corroded containers to the host rock; (iii) hold the containers in place and prevent transfer of excessive stresses to the containers against creep of the host rock; and (iv) transfer the heat generated in the waste to the host rock.

Bentonite is considered to be one of the most promising candidates for use as buffer material in many countries such as Canada (Radhakrishna *et al.* 1989), Sweden (Pusch 1977),

¹Paper presented at the "workshop on Stress-Partitioning in Engineered Clay Barriers," May 29-31, 1991, Duke University, Durham, N.C.

²Revision received March 6, 1992.